Hindawi
Advances in Civil Engineering
Volume 2019, Article ID 9716748, 13 pages
https://doi.org/10.1155/2019/9716748

Research Article

Energy Consumption Analysis of Frozen Sandy Soil and an Improved Double Yield Surface Elastoplastic Model considering the Particle Breakage

Junlin He,[1] **Zhanyuan Zhu**,[1] **Fei Luo**,[1,2] **Yuanze Zhang**,[1] **and Zuyin Zou**[1]

[1]*College of Civil Engineering, Sichuan Agricultural University, Dujiangyan 611830, China*
[2]*College of Post Disaster Reconstruction and Management, Sichuan University, Chengdu 610065, China*

Correspondence should be addressed to Zhanyuan Zhu; 252514862@qq.com

Received 5 July 2018; Accepted 2 December 2018; Published 17 January 2019

Academic Editor: Trung Ngo

The stress-strain relationship of frozen soil is a hot research topic in the field of frozen soil mechanics. In order to study the effect of particle crushing on the stress-strain relationship, a series of triaxial compression tests for frozen sandy soil are performed under confining pressures from 1 to 8 MPa at the temperatures of −3 and −5°C, and the energy consumption caused by particle breakage is analyzed during the triaxial shear process based on the energy principle. It is found that the energy consumption caused by the particle breakage presents a hyperbolic trend with axial strain. In view of the obvious advantages of the double yield surface elastoplastic model in describing soil dilatancy, stress path effect, and stress history influence, a modified double yield surface elastoplastic model for frozen sandy soil is proposed based on the energy principle. The validity of the model is verified by comparing its modeling results with test results. As a result, it is found that the stress-strain curves predicted by this model agree well with the corresponding experimental results under different confining pressures and temperatures.

1. Introduction

Frozen soil, a kind of special geotechnical material, is defined as soil and rock constituents that contain ice with temperatures equal to or below zero [1]. There are 35,760,000 km^2 of permafrost in the world, which accounts for approximately 24% of the world's land area [2]. The permafrost regions are mainly distributed in 48 countries, including Russia, the United States, Canada, and China [3]. With the continuous development of various projects, such as railways, roads, buildings, and energy and water conservation projects in the high-cold areas [4, 5], progressively more frozen soil problems have emerged. Therefore, it is of great value to study the deformation characteristics of frozen soil and constitutive models.

The evolution of yield damage and damage of geomaterials is essentially the process of energy dissipation, which is done by the rearrangement and friction between the particles inside the system [6]. The energy dissipation mechanism is used in many aspects of geomaterials. For example, during the loading process, some researchers use the dissipative energy to judge and evaluate the structural damage or the soil liquefaction [7–9]. The yield function can be established based on the energy principle of establishing the elastoplastic model, and in this respect, this mechanism is more often used, like the classic Cambridge model [10] where the work done by the external force equals the energy dissipated by the friction. Then the energy balance equation is derived from the dilatancy equation under the axial condition, and this is the basis for establishing the yield function. Therefore, a more complete energy dissipation analysis of the material can provide a basis for establishing a more complete and rational constitutive model. Under the normal triaxial loading condition, the axial deviation stress q performs shear deformation work on the sample, and the average principal stress p works on the change of the sample volume. Part of the total input energy will be elastically stored in the sample with the sample undergoing elastic

deformation. The particle breakage (if any in geotechnical materials) will also consume part of the input energy, which should be taken into consideration when establishing the corresponding energy balance equation.

It is found that the frozen sandy soil will also undergo significant particle breakage during triaxial shear [11]. Particle crushing affects the mechanical properties of soil due to the gradation and structural change in soil, which is an important research topic in the field of soil mechanics [12], but there are few studies on the particle crushing of frozen sandy soil and only stay in the experimental stage. However, a great deal of experimental and theoretical research has been devoted to this domain for unfrozen soil and other solid materials, and some constitutive models considering particle breakage have been proposed. The study of the triaxial shear properties of rockfill materials by Marsal [13] has shown that particle crushing is obvious at high confining pressures. Lee [14] has found that the effect of sand particle crushing on the shear strength under drainage conditions is very significant at high confining pressures. Vesic and Clough's [15] studies have shown that particle breakage is more obvious with an increase in stress, while the quantity of the particle breakage of sand is very small when the stress level is less than 0.1 MPa. A triaxial test has been applied to study the effect of particle crushing on the stress-strain characteristics of weathered granite by Miura et al. [16], and the results show that both the number of particle breakages and the particle breakage rate have an effect on the shear strength of sand. Guo Qingguo et al. [17] found that the contact between soil particles is mainly point contact, and the higher the local compressive stress at the contact point during the shearing process is, the more significant the particle shearing phenomenon will be. Meng Jin et al. [18] found that particle breakage of moraine soil has a significant impact on the stress-strain characteristics under high-stress conditions. A damage slip coupling mechanical model based on an elastic damage model and a boundary layer model for calcareous sand were proposed by Sun and Wang [19] to describe the particle breakage and slip. Chavez and Alonso [20] established a constitutive model for coarse-grained soil that considered the effect of particle crushing and wetting. Zhankuan et al. [21] established a relationship between the particle breakage rate and the damage parameters and proposed a constitutive model of the rockfill materials considering the particle breakage based on the rock and soil damage mechanics, which treats rockfill materials as binary media consisting of structures and damaged zones. The relevant constitutive models mainly introduce the particle breakage rate as a parameter into the existing model. Since the particle breakage rate is only an external manifestation of the particulate material under the external load, it is more reasonable to consider the influence of particle breakage on the constitutive relationship from the perspective of energy dissipation given that the influence of the particle breakage has actually been considered in other parameters measured [22].

In the field of energy dissipation considering particle breakage, some research results have been obtained and some constitutive model based on energy principle considering particle breakage has been proposed. Ueng and Chen [23] developed a stress-dilatancy relationship for sand under a triaxial loading condition based on Rowe's minimum energy ratio principle [24]. Furthermore, the energy balance equation considering particle breakage is deduced, and the energy dissipation of sandy soil in triaxial shear process is analyzed. Considering elastic energy storage, Indraratna and Salim [25] established a more complete energy balance equation considering particle crushing based on the energy balance equation established by Ueng et al., In addition, the yield function is established based on the energy balance equation, and the constitutive model considering particle crushing is established by using the non-associated flow rule. Chi and Jia [26] introduced the energy balance equation, which considers particle breakage, into the Rowe constitutive model [24] to correct the tangential bulk modulus. Then, a constitutive model based on the models proposed by Chi and Jia for coarse-grained soils was established to consider the fragmentation of particles proposed by Li [27].

The above constitutive models based on the energy balance equation considering particle breakage are all single-yield surface constitutive models, which can obtain satisfactory results under general loading conditions, while double yield surface models have shown significant advantages in reflecting the soil dilatancy, the stress path influence, and the stress history effect. To date, the Lade model [28], the Vermeer model [29], the elliptic-parabolic double yield surface model [30], and several other double yield surface models have been proposed. However, all of the abovementioned double yield surface models contain many parameters and are difficult to popularize. A double yield surface model has been proposed and developed by Shen [31] for the analysis of several soft soil foundation projects. The model not only overcomes the shortcoming of nonlinear models in describing the dilatancy and the stress-induced anisotropy but also takes into account both the flexibility of the application and the completeness of the theory; thus, the model has been widely used. Clearly, Shen Zhujiang's double yield surface model still has some defects and deficiencies. Some scholars have modified the model to facilitate engineering applications. For example, Zhang et al. [32] used the modified Rowe dilatancy equation to correct the volumetric tangential modulus μ_t based on the triaxial test of the rockfill materials so that the double yield surface model can better describe the stress-strain relationships of the rockfill materials. Luo and Zhang [33] used the newly fitting relations between the volumetric strain and axial strain to modify μ_t and proposed a modified model, which better describes both the dilatancy characteristics of coarse-grained soil under a low confining pressure and the shear shrinkage characteristics under a high confining pressure. Wang Tingbo et al. [34] have applied a formula that relates both the tangential modulus E_t and μ_t and the stress ratio η to correct the E_t and μ_t. These authors have proposed an improved model, which can better describe the shear dilatancy, strength, and deformation characteristics of the rockfill materials.

In order to establish a double yield surface model considering particle breakage for freezing sand based on the

energy principle, firstly, this paper calculates and analyzes the energy dissipation during the triaxial shearing process of frozen sandy soil based on the energy balance equation considering particle breakage. Then, μ_t in Shen Zhujiang's double yield surface model are modified based on the energy principle, and M_t in Shen Zhujiang's double yield surface model are modified based on the softening characteristics of the stress-strain curves of the frozen sandy soil. Thus, a modified double yield surface constitutive model considering particle breakage for frozen sandy soil is established. The modified model not only considers the effect of particle breakage based on energy principle but also has the obvious advantages of Shen Zhujiang's double yield surface model, such as simple form and convenient application.

2. The Phenomenon of Particle Breakage and Its Physical Mechanism in Frozen Sandy Soil

Particle breakage is a basic phenomenon for granular material in a high-stress state. Some experimental results have shown that particle breakage in the frozen soil also exists in a low stress state, and the fracture degree is influenced by the confining pressure, the freeze-thaw cycles, and other factors. Ma et al. [35] used scanning electron microscopy to observe the structure of frozen Lanzhou sand under a confining pressure from 0 to 22 MPa at −5°C. The results indicate that particle breakage occurred when the confining pressure was large and led to a sharp decline in the strength of the frozen soil. Ma et al. [11] found that particle breakage was considerable in frozen sand during the three-axis shear process, and the fracture degree gradually increased with increasing confining pressure. Zheng et al. [36] found that the fracture degree for frozen silt clay particles increased with an increase in the number of freeze-thaw cycles. The content of the grain groups tended to be stable after more than 15 freeze-thaw cycles. Additionally, the particle breakage changed the structure of the frozen soil and significantly influenced the soil's mechanical properties. Figure 1 shows the particle-size distribution curves before and after triaxial compression tests. As can be seen from Figure 1, there are also significant particle breakage phenomena during the triaxial shearing of frozen sandy soil.

For the convenience of research, Guyon and Troadec [37] divided the patterns of particle breakage into three types: (a) rupture, i.e., the original particle becomes smaller particles with an approximately equal particle size; (b) fracture, i.e., the original particle becomes a larger particle and other smaller particles; and (c) grind, i.e., the original particles remain almost unchanged, but the surface produces fine particles due to grinding. The three types are shown in Figure 2. To reveal the particle breakage mechanism of frozen sandy soil, the frozen sandy soil is considered a composite granular material consisting of a soil particle skeleton, gel ice, and pore ice. The contact between particles in frozen sandy soil can be seen as point by surface or point-by-point interaction. The contact model is shown in Figure 3. The contact area between the particles is very small when compared with the specific surface area of the particles; thus, the stress caused by a small external load at the contact

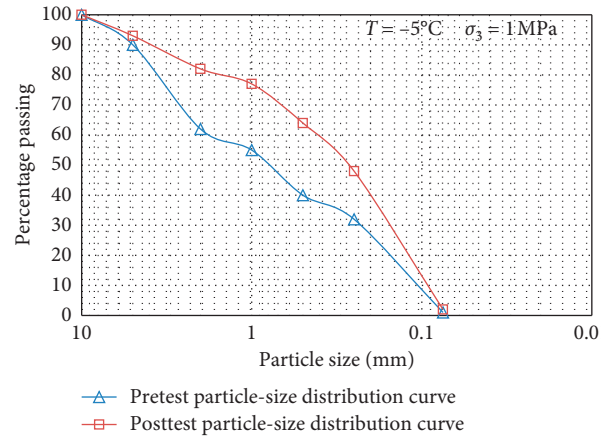

Figure 1: Particle-size distribution curves before and after triaxial compression tests.

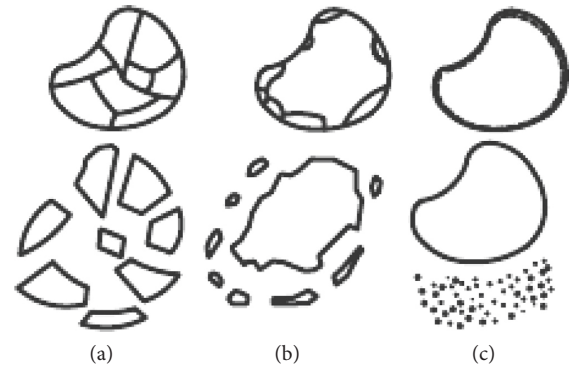

Figure 2: Schematic diagrams of the types of particle breakage. (a) Rupture. (b) Fracture. (c) Grind.

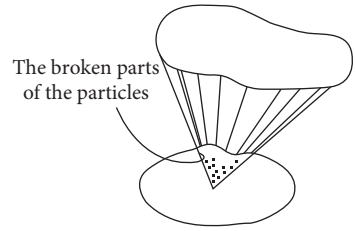

Figure 3: Physical model of particle breakage with point and surface contact.

point may also be very large. For more regular particles in frozen sandy soil, the form of particle breakage is generally the first and the second type shown in Figure 2 under a compression process, while the third form occupies a large proportion during the shearing process. For irregular particles, the stress concentration is generally broken at the edges and corners. As the shearing process progresses, the contact area between the particles gradually becomes larger, so the stress at the contact point gradually decreases, and it is difficult to break the particles. Based on this understanding and previous research results, the general law of frozen soil particle crushing is summarized as follows: (1) even a small stress can cause particle breakage in frozen sandy soil; (2)

with an increasing degree of particle breakage, the contact area between the particles gradually becomes larger, and the frequency of particle crushing tends to decelerate; (3) when the strain increases to a certain extent, the slip and rolling actions between particles are dominant, and particle breakage does not occur again.

3. Energy Consumption Analysis for Frozen Sandy Soil during the Triaxial Shear Process

To study the effect of particle breakage energy consumption on stress-strain relationships of frozen sandy soil, a series of triaxial compression tests are performed under confining pressures from 1 to 8 MPa at the temperatures of −3 and −5°C.

3.1. Energy Balance Equation considering Particle Breakage. Soil particles, cemented ice, and pore ice in frozen soil are all considered granular materials. The particles will deform, slip, roll, and break during triaxial shearing. Ueng and Chen [23] analyzed the force and deformation of granular materials during the triaxial shearing process from a mesoscopic viewpoint based on Rowe's minimum energy ratio principle [24]. Therefore, the energy balance equation considering particle breakage is derived and can be rewritten as

$$\sigma_1 d\varepsilon_1 + \sigma_3 (d\varepsilon_v - d\varepsilon_1)\tan^2\left(\frac{\pi}{4} + \frac{\varphi_f}{2}\right) = dE_B(1 + \sin\ \varphi_f), \tag{1}$$

where σ_1 and σ_3 are the first and third principal stresses; ε_1, ε_v, and ε_s are the axial strain, the body strain, and the generalized shear strain, respectively; and φ_f is the friction angle of the soil.

In the p-q stress space, there are

$$\left.\begin{aligned} \sigma_1 &= p + \frac{2q}{3}, \\ \sigma_3 &= p - \frac{q}{3}, \\ d\varepsilon_s &= d\varepsilon_1 - \frac{d\varepsilon_v}{3}, \end{aligned}\right\} \tag{2}$$

$$\tan^2\left(\frac{\pi}{4} + \frac{\varphi_f}{2}\right) = \frac{1 + \sin\ \varphi_f}{1 - \sin\ \varphi_f} = \frac{3 + 2M_{cr}}{3 - M_{cr}}, \tag{3}$$

where p and q are the average stress and generalized shear stress, respectively, and M_{cr} is the critical-state stress ratio. Substituting (2) and (3) into (1), we can obtain the following:

$$\begin{aligned} pd\varepsilon_v^p + qd\varepsilon_s^p = M_{cr} pd\varepsilon_s^p + \frac{2q - 3p}{9} M_{cr} d\varepsilon_v^p \\ + \frac{(3 - M_{cr})(6 + 4M_{cr})}{3(6 + M_{cr})} dE_B. \end{aligned} \tag{4}$$

Using the assumption of the Cambridge model that does not consider elastic shear strain [10], equation (4) can be written as

$$\begin{aligned} pd\varepsilon_v + qd\varepsilon_s = pd\varepsilon_v^e + M_{cr} pd\varepsilon_s + \frac{2q - 3p}{9} M_{cr} d\varepsilon_v^p \\ + \frac{(3 - M_{cr})(6 + 4M_{cr})}{3(6 + M_{cr})} dE_B. \end{aligned} \tag{5}$$

For the convenience of presentation, some expressions are written as

$$\left.\begin{aligned} E_T &= pd\varepsilon_v + qd\varepsilon_s, \\ E_G &= pd\varepsilon_v^e, \\ E_F &= M_{cv} pd\varepsilon_s, \\ E_D &= \frac{2q - 3p}{9} M_{cv} d\varepsilon_v^p, \\ E_B &= \frac{(3 - M_{cr})(6 + 4M_{cr}) dE_B}{3(6 + M_{cr})}. \end{aligned}\right\} \tag{6}$$

The total input energy E_T is converted into four parts: the elastic energy storage E_G, the friction energy consumption E_F, the dilatancy energy consumption E_D, and the particle breakage energy consumption E_B. Notably, equation (5) can be degenerated into the Rowe dilatancy equation [24] when the elastic energy storage and particle crushing energy consumption are not considered. Additionally, equation (5) can be reduced to the Cambridge model dilatancy equation [10] when the dilation work and particle breakage energy consumption are not considered.

To study the effect of particle crushing on the stress-strain relationship, it is necessary to use equation (5) to determine the energy consumption of E_B during triaxial shearing. The key to determining the energy dissipation of particle breakage by using (5) is to determine the elastic volume strain and the critical-state stress ratio M_{cr}, while the other parameters can be calculated by the trapezoid integral formula through the experimental data.

The rebound test results of frozen sandy soil are shown in Figure 4, and the elastic volumetric strain can be calculated by the equation suggested by El Sohby [38]. The formula is as follows:

$$\varepsilon_v^e = k(p)^l, \tag{7}$$

where k and l are the experimental parameters, which can be determined by the test data.

During the triaxial shearing process, the soil and ice particles for frozen sandy soil are continuously broken. The particle breakage changes the contact state and area between adjacent particles. Therefore, the stress ratio increases with increasing shear strain. However, with a decrease in the particle dimension, the particle breakage becomes increasingly difficult; thus, the stress ratio decreases. Based on the test results and the above analysis, the relationship between the stress ratio of the frozen sandy soil and the shear strain can be shown as follows:

$$M = \frac{a\varepsilon_s}{b + \varepsilon_s}, \tag{8}$$

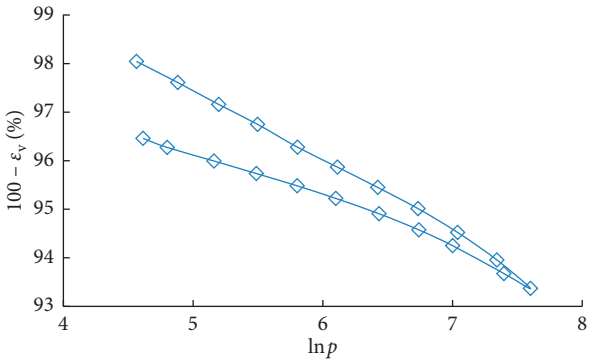

Figure 4: Frozen sandy soil rebound test results.

where a and b are the test parameters, which can be obtained by fitting the test data. After fitting the test data, the relationship between the parameters b and σ_3 can be expressed as follows:

$$b = s\left(\frac{\sigma_3}{p_a}\right) + t, \tag{9}$$

where s and t are the fitting parameters.

Substituting (9) into (8), we obtain

$$M = \frac{a\varepsilon_s}{s + t\sigma_3 + \varepsilon_s}, \tag{10}$$

where the parameter σ_3 reflects the influence of the confining pressure on the stress ratio.

The internal friction angle of soil is closely related to the interaction between the particles and the smooth surface. For frozen sandy soil, the body stress will increase the biting effect among the particles, and both the shear stress and the body stress will cause the melting of the ice, which will produce smooth particle surfaces. Hence, the friction angle of frozen soil varies with the stress state. It is assumed that the friction angle is proportional to the stress ratio, and the relationship between the friction angle and stress ratio in the loading process can be expressed as

$$\tan^2\left(\frac{\pi}{4} + \frac{\varphi}{2}\right) = \frac{1 + \sin\varphi}{1 - \sin\varphi} = \frac{3 + 2M}{3 - M}. \tag{11}$$

From equations (1), (4), and (11), we can obtain

$$\begin{aligned} &\sigma_1 d\varepsilon_1 + \sigma_3\left(d\varepsilon_v - d\varepsilon_1\right) \\ &\cdot \tan^2\left(\frac{\pi}{4} + \frac{\varphi}{2}\right) = dE_B\left(1 + \sin\varphi\right), \end{aligned} \tag{12}$$

$$\begin{aligned} p\, d\varepsilon_v + q\, d\varepsilon_s = {} & p\, d\varepsilon_v^e + Mp\, d\varepsilon_s + \frac{2q - 3p}{9} M\, d\varepsilon_v^p \\ & + \frac{(3 - M)(6 + 4M)}{3(6 + M)} dE_B, \end{aligned} \tag{13}$$

where the internal friction angle φ in the formula is an ever-changing parameter during the shearing process.

3.2. Energy Transformation Mechanism of Frozen Sandy Soil during the Three-Axis Shearing Process. The total input energy can be gradually transformed into elastic energy storage, dilatancy work, particle crushing energy dissipation, and friction energy dissipation; energy consumption varies during the shearing process. To study the change in and the mutual transformation mechanism of energy consumption in the different parts during the shearing process, the energy balance equation considering the particle breakage expressed by equation (13) is applied to study the change in energy consumption. The energy consumption ratio along with the axial strain during the loading process is shown in Figure 5. From Figure 4, both the work caused by dilatancy and the proportion of the work are small since the dilatancy of frozen soil during the whole shearing process is not obvious. During the initial loading period, the particle slip and rolling action are not significant, and a small number of particles are broken because of the low stress level. As a result, the total input energy can be transformed into elastic energy storage and a small amount of particle crushing energy consumption. As the stress level increases, the particle breakage is particularly significant because particles are mainly contacted by dots or dots and surfaces. Therefore, the particle breakage energy and the ratio of particle breakage to the total energy significantly increase. Meanwhile, particle sliding and rolling are also gradually enhanced; thus, the friction energy consumption and the ratio of that to total energy correspondingly increase, but the elastic energy storage ratio rapidly decreases due to an increase in the total input energy. Along with a further increase in the shear load, the amount of particle breakage increases by deceleration due to an increase in the contact area between particles; therefore, the particle breakage energy gradually increases, but the energy dissipation ratio of the particle breakage decreases due to an increase in the total input energy. During this process, particle sliding and rolling are dominant, so the friction energy consumption and friction energy consumption ratio gradually increase. As the stress reaches the maximum, the particle breakage stopped completely, and the particle crushing energy consumption correspondingly reached the maximum, while the energy consumption ratio of the particle breakage is gradually reduced because of an increase in the total input energy. At this point, the critical state appears and both the friction energy consumption and friction energy consumption ratio tend to be stable.

3.3. Relationship between Particle Crushing Energy Consumption and Axial Strain. The particle crushing energy consumption and the energy dissipation ratio under test processing conditions can be determined by equations (7), (10), and (13). During the initial loading stage, the particle breakage can be caused by smaller loads, which may lead to greater stress because the particles are mainly contacted by dots or dots and surfaces. However, the amount of particle breakage is less, and the energy consumption ratio of the particle breakage is relatively large because of less total input energy. As the stress level increases, the amount of particle breakage increases by deceleration due to an increase in the contact area between particles. As a result, the particle breakage energy is still increasing, but the ratio of particle

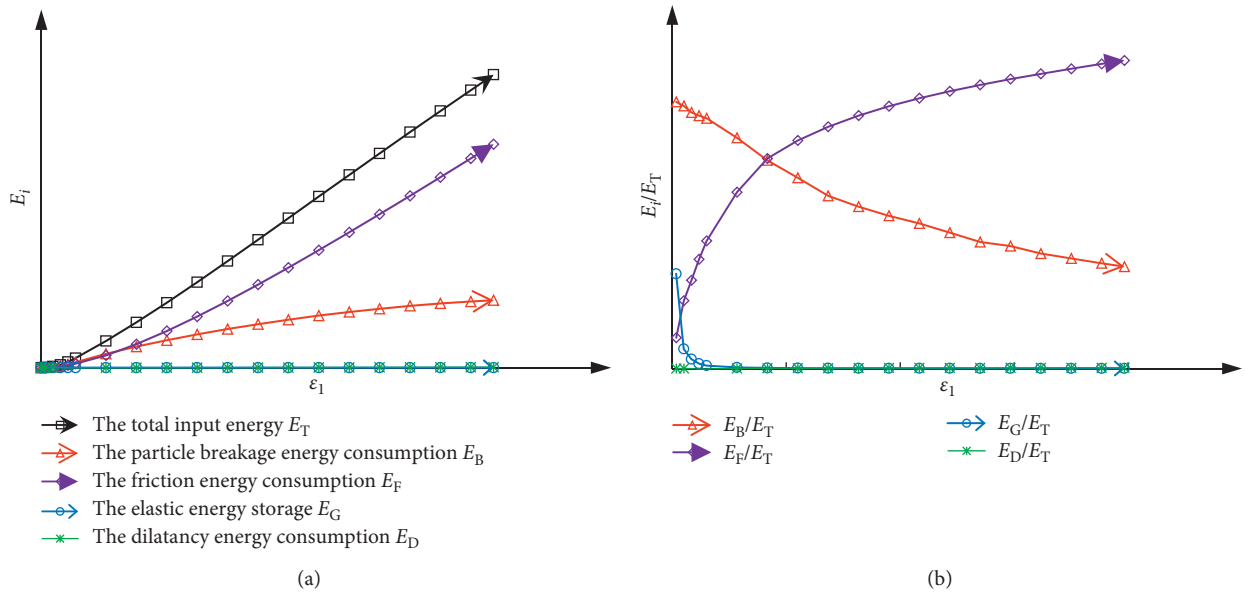

FIGURE 5: Schematic diagram of changes in (a) energy consumption and (b) the ratio of the energy consumption to total input energy during the loading process.

breakage to the total energy gradually decreases due to an increase in the total input energy. As the stress reaches the maximum, the particle breakage stops completely, the particle crushing energy consumption correspondingly reaches the maximum, and the energy consumption ratio of particle breakage is stable.

In addition, the particle crushing energy consumption during the test process is significantly affected by the confining pressures. This law, namely, that the particle crushing energy consumption increases with increasing confining pressures during the whole loading process at the same axial strain, as shown in Figure 6, is consistent with the research results of Zhankuan et al. [21] and Hassanlourad et al. [39]. It is generally believed that the higher the confining pressure is, the stronger the particles confinement is. Therefore, if the particles bear greater stress at the same strain, then the particle breakage is more prone to occur, and the amount of particle breakage increases. In addition, the particle breakage will further restrict particle sliding and rolling; therefore, the friction energy consumption decreases with increasing confining pressure.

The trends of the various energy consumptions with axial strain at different temperatures and different confining pressures are basically the same. The curve of the particle breakage energy consumption is shown in Figure 6, and the relationship between the particle breakage energy consumption and the axial strain may be approximated by a hyperbola, which can be rewritten in the following form:

$$E_B = \frac{\varepsilon_1}{e\varepsilon_1 + f}, \tag{14}$$

where both e and f are the experimental parameters.

It is found that the relationships between the parameters f and σ_3 at different temperatures are linear and can be written as

$$f = a_1\left(\frac{\sigma_3}{p_a}\right) + b_1, \tag{15}$$

where a_1 and b_1 are the fitting parameters.

Taking the derivative of equation (14), we can obtain

$$\frac{dE_B}{d\varepsilon_1} = \frac{f}{(f + e\varepsilon_1)^2}. \tag{16}$$

4. The Modified Double Yield Surface Model considering Particle Breakage

The nonlinear elastic model cannot describe the dilatancy of soil, and the single-yield surface elastoplastic model cannot be applied to engineering problems under high confining pressure or a reduction in the confining pressure. Roscoe [40] presented the concept of a double yield surface when the modified Cambridge model was proposed. Afterwards, increasingly more individuals were aware of the necessity of introducing the concept of the double yield surface, and some scholars have put forward some double yield surface models, but these models have many parameters and have been difficult to popularize. A double yield model is proposed based on the study of Shen [31]. The model has been successfully applied to the design of multiple earth rockfill dams and has broad application prospects.

4.1. Shen Zhujiang's Double Yield Surface Model. Shen Zhujiang's double yield surface model is proposed based on a new hardening theory-equivalent stress theory; that is, an equivalent triaxial stress (σ_1, σ_3) can be found for each stress

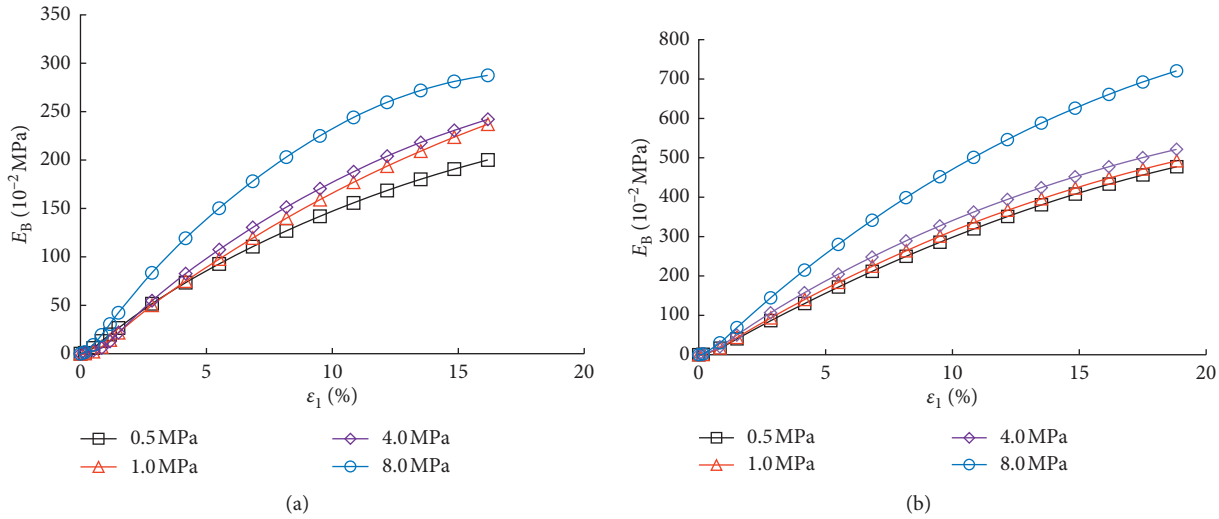

Figure 6: Relation curve of energy consumption of particle breakage and shear strain. (a) $T = -3^{\circ}C$. (b) $T = -5^{\circ}C$.

$\{\sigma\}$, and it is assumed that the plastic modulus measured under the triaxial stress state can be directly used for other stress states [31]. In this theory, the yield surface is only used as a criterion for additional unloading, and it is not necessary to use it to calculate the hardening modulus. Shen Zhujiang's double yield surface model uses two yield surfaces, namely, a volume yield surface and a shear yield surface, to describe the yield characteristics, and the yield surface equation is expressed as

$$\left.\begin{aligned} f_1 &= p^2 + r^2 q^2, \\ f_2 &= \frac{q^2}{p}, \end{aligned}\right\} \tag{17}$$

where q is the generalized shear stress, p is the mean principal stress, and R and s are the material parameters.

When the normal flow rule is adopted, the elastic-plastic stress-strain relationship can be expressed as

$$\{\Delta\varepsilon\} = [D]_c^{-1}\{\Delta\sigma\} + A_1\left\{\frac{\partial f_1}{\partial\sigma}\right\}\Delta f_1 + A_2\left\{\frac{\partial f_2}{\partial\sigma}\right\}\Delta f_2, \tag{18}$$

where A_1 and A_2 are the plastic coefficients that correspond to the yield surfaces f_1 and f_2, respectively.

In the conventional triaxial test stress state, A_1 and A_2 obtained by (17) and (18) can be, respectively, expressed as

$$\left.\begin{aligned} A_1 &= \frac{1}{4p^2}\,\frac{\eta\left((9/E_t) - (3\mu_t/E_t) - (3/G_e)\right) + 3s\left((3\mu_t/E_t) - (1/B_e)\right)}{3\left(1 + 3\eta r^2\right)\left(s + \eta^2 r^2\right)}, \\ A_2 &= \frac{p^2 q^2}{q^{2s}}\,\frac{\left((9/E_t) - (3\mu_t/E_t) - (3/G_e)\right) - 3r^2\eta\left((3\mu_t/E_t) - (1/B_e)\right)}{3\left(3s - \eta\right)\left(s + \eta^2 r^2\right)}, \end{aligned}\right\} \tag{19}$$

where G_e and B_e are the test parameters and E_t and μ_t are the tangent modulus and the volume tangent modulus, respectively, which can be expressed as

$$\left.\begin{aligned} E_t &= \frac{d(\sigma_1 - \sigma_3)}{d\varepsilon_1}, \\ \mu_t &= \frac{d\varepsilon_v}{d\varepsilon_1}. \end{aligned}\right\} \tag{20}$$

It can be seen from (18) and (19) that the determination of E_t and μ_t is the key to determining the stress-strain relationships:

$$E_t = \left(1 - R_f\frac{(\sigma_1 - \sigma_3)(1 - \sin\varphi)}{2\sigma_3\sin\varphi + 2c\cos\varphi}\right)K \cdot p_a\left(\frac{\sigma_3}{p_a}\right)^n, \tag{21}$$

where P_a is the standard atmospheric pressure, K is the uniform initial elastic modulus coefficient, n is the power of the initial elastic modulus with confining pressure, R_f is the failure ratio, and c and φ are the cohesion and internal friction angle of the material, respectively.

A parabola is used to describe the relationship between ε_v and ε_1, which can be expressed as

$$\varepsilon_v = \varepsilon_{vd}\left(2 - \frac{\varepsilon_1}{\varepsilon_d}\right)\frac{\varepsilon_1}{\varepsilon_d}, \tag{22}$$

where ε_{vd} is the maximum shrinkage strain and ε_v is the body strain corresponding to the maximum shrinkage strain, as shown in Figure 4.

Substituting (22) into (20), μ_t can be obtained:

$$\mu_t = 2c_d\left(\frac{\sigma_3}{p_a}\right)^{n_d}\frac{E_i R_f S_1}{\sigma_1 - \sigma_3}\cdot\frac{1 - R_d}{R_d}\left(1 - \frac{R_f S_1}{1 - R_f S_1}\cdot\frac{1 - R_d}{R_d}\right), \tag{23}$$

where E_i is the initial elastic modulus, S_1 is the stress level parameter, c_d is the maximum body strain when the confining pressure is one atmosphere, n_d is the power of the body strain that changes with the confining pressure, and R_d is the stress ratio that corresponds to the maximum body

strain. The three parameters c_d, n_d, and R_d can be fitted by the test data, and the fitted formula is as follows:

$$\varepsilon_{vd} = c_d\left(\frac{\sigma_3}{p_a}\right)^{n_d},$$
$$R_d = \frac{(\sigma_1-\sigma_3)_d}{(\sigma_1-\sigma_3)_{ult}}, \tag{24}$$

where $(\sigma_1-\sigma_3)_d$ is the deviation stress that corresponds to the maximum shrinkage of the sample and $(\sigma_1-\sigma_3)_{ult}$ is the limit value of the deviation stress. The physical meaning of these parameters is shown in Figure 7.

There are few parameters in Shen Zhujiang's double yield surface model, and the parameters can be determined through conventional triaxial tests. However, the relationship between the deviation stress and the axial strain in Shen Zhujiang's double yield surface model can be approximated by a hyperbola so that the model cannot describe the strain softening phenomenon. In addition, the parabola is used to describe the relationship between the volumetric strain and axial strain. Considerable experimental data have proven that the model has a large amount of bulk expansion and the calculated amount of the bulk expansion is large when the strain is large [31–33], and the model does not consider the impact of particle breakage. Therefore, a modified model is proposed on the basis of Shen Zhujiang's double yield surface model, which takes frozen sandy soil as the research object to reflect the strain softening, dilatancy, elastoplastic, and particle breakage characteristics of the frozen soil during the three-axis shear process.

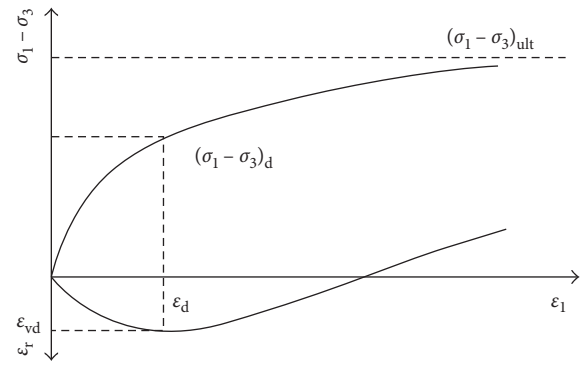

Figure 7: Schematic diagram of stress-strain curves of the Shen Zhujiang double yield surface model.

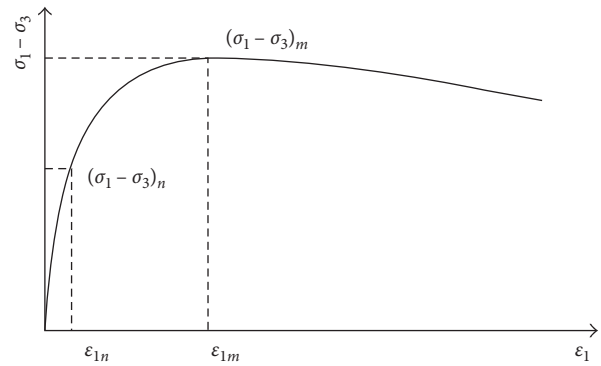

Figure 8: Schematic diagram of physical meaning of some parameters.

4.2. Correction of the Tangential Modulus E_t. Based on the results of the triaxial tests, it was found that E_t of the frozen sandy soil in the triaxial shear process first gradually decreases, when the peak stress is reached, E_t is 0, and the strain softening phase E_t is negative. To describe the softening characteristics of the stress-strain curves of the frozen sandy soil and considering the effects of the stresses $(\sigma_1-\sigma_3)_m$, $(\sigma_1-\sigma_3)_n$, and the corresponding strains ε_{1m}, ε_{1n} at the boundary points of the stress-strain curve, the relationship between stress and strain of the frozen sandy soil is suggested as

$$\sigma_1-\sigma_3 = \frac{\varepsilon_1}{h+i\varepsilon_1+j\varepsilon_1^2}, \tag{25}$$

$$\left.\begin{aligned} h &= \frac{100}{E_0},\\ i &= \frac{1}{(\sigma_1-\sigma_3)_m}-\frac{100}{E_0\varepsilon_{1m}}+\left(\frac{1}{(\sigma_1-\sigma_3)_n}-\frac{2000}{(E_0\varepsilon_{1n})}\right)\cdot\frac{\varepsilon_{1n}}{20\varepsilon_{1m}},\\ j &= \frac{100}{E_0\varepsilon_{1m}^2}\left(0.8+\frac{2\varepsilon_{1n}}{\varepsilon_{1m}}\right). \end{aligned}\right\} \tag{26}$$

The physical meaning of the parameters ε_{1m} and ε_{1n} are shown in Figure 8. The experimental results show that when the temperature and confining pressure are different, the value of ε_{1n} remains almost constant, which is approximately 1%, which is convenient for the calculation, and takes $\varepsilon_{1n}=1\%$ under different conditions.

Taking the derivative of (25), we obtain

$$E_t = \frac{-l\varepsilon_1^2+m}{\left(l\varepsilon_1^2+n\varepsilon_1+m\right)^2}. \tag{27}$$

Equation (27) is introduced into Shen Zhujiang's double yield surface model to correct E_t, which overcomes the defect that the original model cannot describe strain softening phenomenon.

4.3. Correction of the Volume Tangent Modulus μ_t. The dilatancy equation for particle crushing after the correction for frozen moraine soil is represented by equation (12), where the incremental energy consumption dE_B of particle crushing is determined by (14) and the friction angle φ is given by (8) and (21). Equation (12) is introduced into μ_t expression in Shen Zhujiang's double yield surface model to obtain

$$\mu_t = \frac{d\varepsilon_v}{d\varepsilon_1} = 1-\frac{(3-M)\sigma_1}{(3+2M)\sigma_3}+\frac{(6-2M)f}{\left(f+e\varepsilon_1\right)^2(6+M)\sigma_3}, \tag{28}$$

where M is determined by (10).

The dilatancy equation for particle crushing after the frozen sand soil correction was introduced into Shen Zhujiang's double yield surface model to correct its μ_t so that the model considers the impact of particle breakage when calculating μ_t. This consideration greatly enhances the model; thus, it has better applicability to frozen sand soil.

5. Parameter Determination and Initial Verification

To verify the correctness of the model, the conventional three-axis test results for frozen sandy soil were used to confirm the parameters and verify accuracy. The test control temperatures are −3°C and −5°C, and the confining pressures are 0.5 MPa, 1 MPa, 4 MPa, and 8 MPa.

5.1. Model Parameter Determination. The proposed modified double yield surface model involves 9 parameters, which are divided into two groups. All of these parameters can be determined by conventional triaxial tests. The specific determination methods are as follows.

5.1.1. Parameters Related to the Tangent Modulus E_t. The physical meaning of the parameters l, m, and n is known from equation (26) and Figure 8. The values of the parameters l and n are calculated from equation (26) based on the test data, and the value of parameter m is determined by fitting the test data. The determined parameter values related to E_t are shown in Table 1.

5.1.2. Parameters Related to the Tangent Modulus of the Volume μ_t. The values of the parameters a, s, and t are obtained by fitting equations (8) and (9) based on the test data, and the values of the parameters e, a_1, and b_1 are obtained by fitting equations (14) and (15) based on the test data. The determined parameter values related to the volume tangent modulus μ_t are shown in Table 2.

5.2. Comparison between Model Preliminary Verification and Fitting Effect. To ensure that the simulation and experimental results are comparable, the comparison results are only shown under confining pressures from 1 MPa to 8 MPa at −3°C and −5°C due to space limitations.

Conveniently, the original double yield surface model proposed by Shen [31] is represented by M1, the double yield surface model proposed by Zhang [32] based on the modified Rowe dilatancy equation is represented by M2, and the proposed double yield surface model in this paper is represented by M3.

Both the simulation and experimental results of the stress-strain curves for frozen sandy soil are shown in Figure 9 and Figure 10 at the same temperature and confining pressure. The simulation results of both the M1 and M2 models are consistent because the hyperbolic curve in the Duncan–Chang model is used to describe stress-strain curves in both the M1 and M2 models. The contrast results show that the strain softening phenomenon of frozen sand soil cannot be described by the M1 and M2 models. The simulated values of the M1 and M2 models are larger at the initial loading stage and the strain softening stage, while the strain softening characteristics of frozen sandy soil can be described by the M3 model, which is more accurate than both the M1 model and the M2 model in describing the stress-strain curve relationships.

Table 1: Parameters related to the tangent modulus E_t.

T (°C)	σ_3 (MPa)	h	i	j
−3	0.5	0.2501	0.2283	0.0012
	1.0	0.2	0.2	0.0
	4.0	0.2	0.2	0.0
	8.0	0.2	0.2	0.0
−5	0.5	0.2	0.2	0.0
	1.0	0.2	0.2	0.0
	4.0	0.1	0.2	0.0
	8.0	0.1	0.2	0.0

Table 2: Parameters related to the volume tangent modulus μ_t.

T (°C)	σ_3 (MPa)	a	s	t	e	a_1	b_1
−3	0.5	2.1	0.1472	4.0229	0.0015	−0.0030	0.0535
	1.0	1.8					
	4.0	0.8					
	8.0	0.5					
−5	0.5	2.3	0.6281	5.1071	0.0006	−0.0015	0.0283
	1.0	1.9					
	4.0	0.9					
	8.0	0.5					

A comparison of the body variation curves between the simulation results based on the M1, M2, and M3 models and the test results is made, and the contrast results are shown in Figures 11 and 12. As seen from Figures 11 and 12, the simulation results of the M1 model are large and greatly deviate from the experimental results. The simulation results of the M2 model are closer to the experimental results than those of the M1 model since the M2 model is corrected on the basis of the M1 model. However, the results of the simulated bulge are also large under certain confining pressures. The relationships between the volumetric strain and axial strain of the frozen moraine are better simulated by the M3 model, which better conforms with the experimental results.

The comparison results show that the proposed model is more accurate than the original Shen Zhujiang's double yield surface model and the modified model proposed by Zhang Bingyin. It is necessary to illustrate that the proposed model is only verified by the test results of frozen sand soil under confining pressures of 0.5, 1, 4, and 8 MPa and at a temperature of −3 and −5°C. Furthermore, it is necessary to study the application range and parameter optimization of the model in depth.

6. Conclusions

(1) During the three-axis shear process for frozen sandy soil, the total input energy can be transformed into four parts: elastic energy storage, dilatancy energy consumption, particle breakage energy consumption,

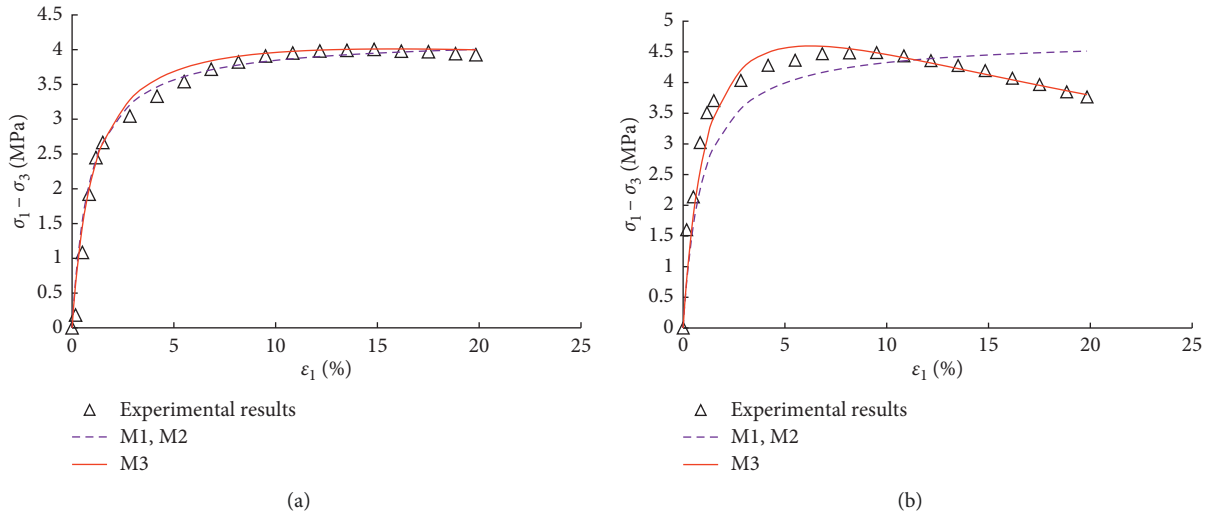

Figure 9: Deviatoric stress-strain relationship fitting results for each model at −3°C. (a) $T = -3$°C, $\sigma 3 = 1.0$ MPa. (b) $T = -3$°C, $\sigma 3 = 8.0$ MPa.

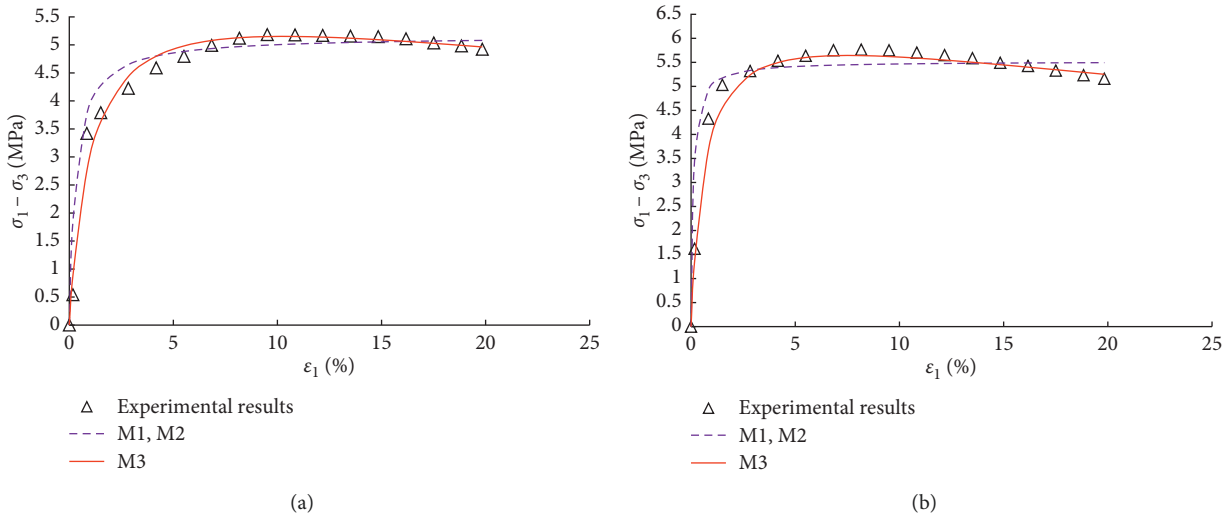

Figure 10: Deviatoric stress-strain strain relationship fitting results for each model at −5°C. (a) $T = -5$°C, $\sigma_3 = 1.0$ MPa. (b) $T = -5$°C, $\sigma_3 = 8.0$ MPa.

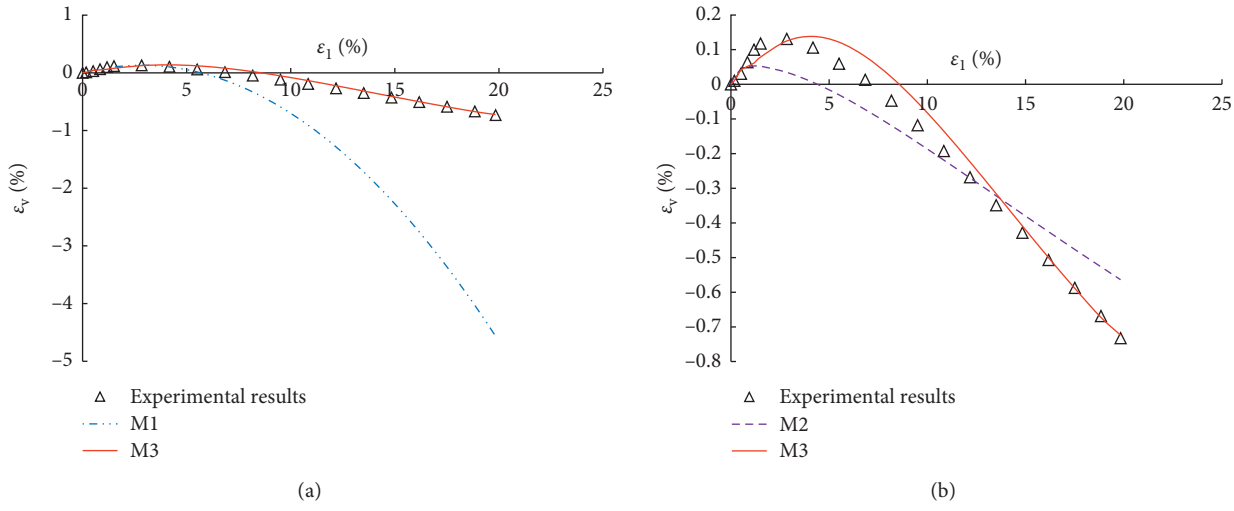

Figure 11: Continued.

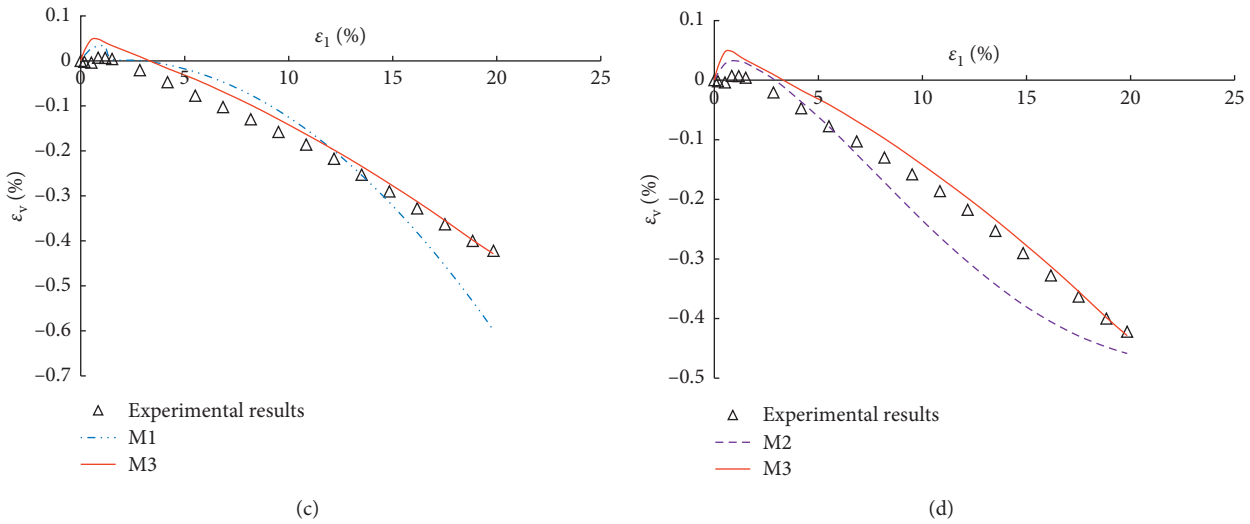

FIGURE 11: Volumetric strain-axial strain relationship fitting results for each model at −3°C. Comparison between experimental results and calculated results of (a) M1 and M3 ($T = -3$°C, $\sigma_3 = 1.0$ MPa), (b) M2 and M3 ($T = -3$°C, $\sigma_3 = 1.0$ MPa), (c) M1 and M3 ($T = -3$°C, $\sigma_3 = 8.0$ MPa), and (d) M2 and M3 ($T = -3$°C, $\sigma_3 = 8.0$ MPa).

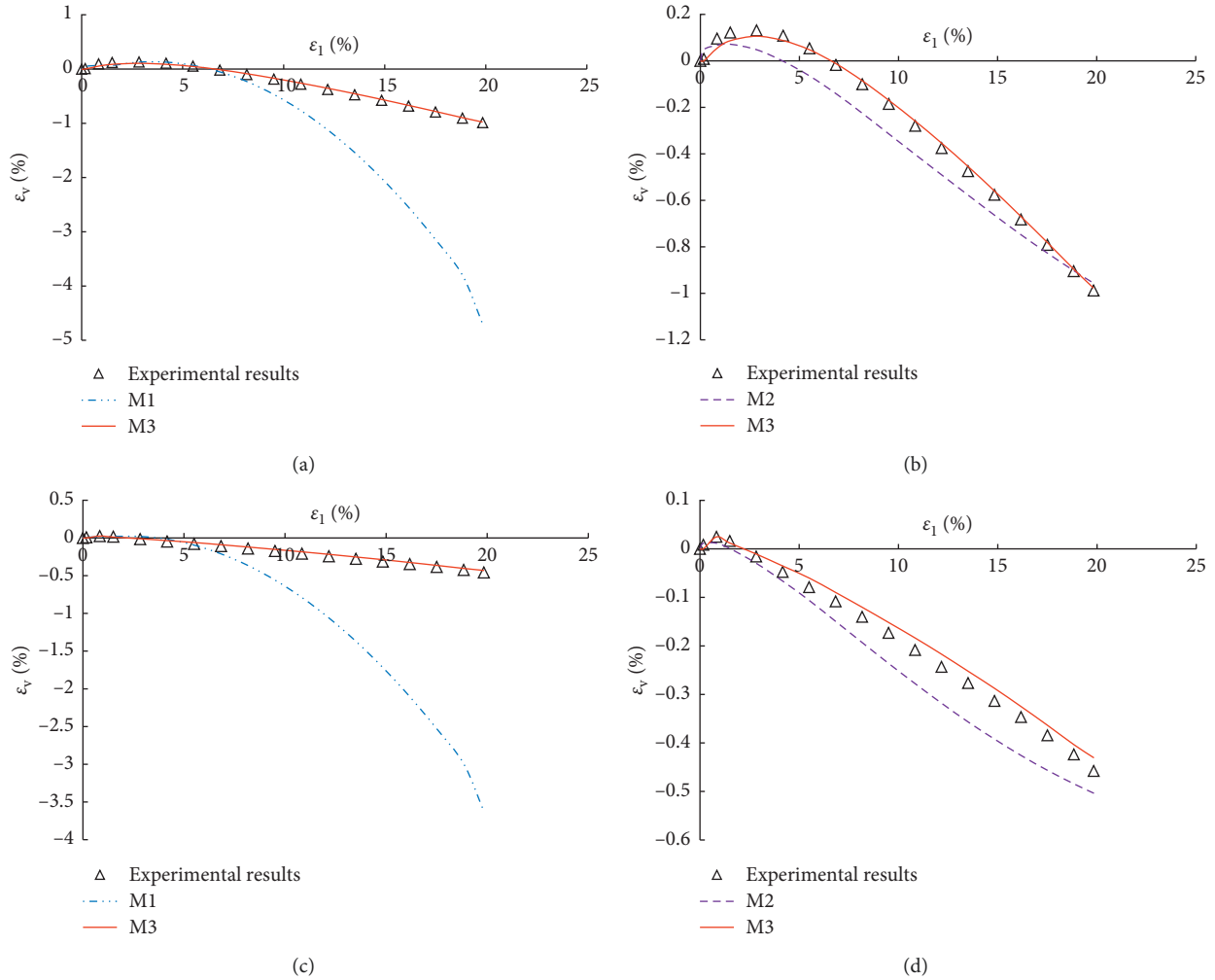

FIGURE 12: Volumetric strain-axial strain relationship fitting results for each model at −5°C. Comparison between experimental results and calculated results of (a) M1 and M3 ($T = -5$°C, $\sigma_3 = 1.0$ MPa), (b) M2 and M3 ($T = -5$°C, $\sigma_3 = 1.0$ MPa), (c) M1 and M3 ($T = -5$°C, $\sigma_3 = 8.0$ MPa), and (d) M2 and M3 ($T = -5$°C, $\sigma_3 = 8.0$ MPa).

and friction energy consumption. During the triaxial shearing process, the total input energy gradually transforms into elastic energy storage, dilatancy energy consumption, particle crushing energy consumption, and friction energy consumption. The proportion of the shear expansion to the total input energy during the whole shearing process is very small. The proportion of the elastic energy storage to the total input energy is larger in the initial stage and rapidly decreases to a small value as the shearing process progresses. The friction energy consumption and the proportion of the friction energy consumption to the total input increase with the shearing process. The energy consumption of particle breakage presents a decelerating growth trend during the whole shearing process, and the proportion of the particle breakage energy consumption to the total input energy rapidly increases within a small strain range at the initial stage of loading and gradually decreases with loading. In addition, the larger the confining pressure is, the greater the energy consumption of particle breakage will be.

(2) Based on the deformation characteristics and the energy principle of frozen sandy soil, E_t and μ_t in Shen Zhujiang's double yield surface model and thereby a double yield surface constitutive model suitable for frozen sandy soil are proposed. The calculation results of Shen Zhujiang's double yield surface model, the modified model proposed by Zhang Bingyin, and the proposed model are compared with the experimental results. The results show that the calculated results of the proposed model are the closest to the test results, which better reflect the strain softening and dilatancy characteristics of frozen sandy soil.

Data Availability

Since the experiment was completed with the support of Sichuan Agricultural University, the data used to support the results of this study can be obtained from the responsible person and the author upon request.

Conflicts of Interest

The authors declare that they have no conflicts of interest.

Acknowledgments

This work was supported by the National Natural Science Foundation of China (41701063 and 41672304) and Student's Platform for Innovation Training Program (4054662 and 04070055).

References

[1] T. Zhang, Z. Youwu, G. Dongxin, Q. Guoqing, C. Guodong, and L. Shude, "Geocryology in China," *Arctic, Antarctic, and Alpine Research*, vol. 33, no. 2, p. 245, 2001.

[2] G. H. Brown, "The periglacial environment (second edition)," *Applied Geochemistry*, vol. 13, no. 2, pp. 281-282, 1998.

[3] T. J. Zhang, M. A. Parsons, and R. G. Barry, "Statistic of global permafrost distribution," in *Proceedings of Asian Conference on Permafrost (Abstract)*, pp. 7-8, Lanzhou, China, August 2006.

[4] X. Wang and Z. Zhang, "Engneering in cold region and mechanics of frozen-thawymedia," *Earth Science Frontiers*, vol. 7, no. B08, pp. 99–104, 2000.

[5] W. Ma and D. Wang, "Studies on frozen soil mechanics in China in past 50 years and their prospect," *Chinese Journal of Geotechnical Engineering*, vol. 34, no. 4, pp. 625–640, 2012.

[6] Y. Yang, Y. Lai, S. Li et al., "Experimental study of deformation failure and energy properties of frozen silt under triaxial compression," *Rock and Soil Mechanics*, vol. 31, no. 11, pp. 3505–3510, 2010.

[7] S. Nemat-Nasser and A. Shokooh, "A unified approach to densification and liquefaction of cohesionless sand in cyclic shearing," *Canadian Geotechnical Journal*, vol. 16, no. 4, pp. 659–678, 1979.

[8] M. F. Ishac and A. C. Heidebrecht, "Energy dissipation and seismic liquefaction in sands," *Earthquake Engineering and Structural Dynamics*, vol. 10, no. 1, pp. 59–68, 1982.

[9] K. T. Law, Y. L. Cao, and G. N. He, "An energy approach for assessing seismic liquefaction potential," *Canadian Geotechnical Journal*, vol. 27, no. 3, pp. 320–329, 1990.

[10] K. H. Roscoe, A. N. Schofield, and A. Thurairajah, "Yielding of clays in states wetter than critical," *Géotechnique*, vol. 13, no. 3, pp. 211–240, 1963.

[11] L. Ma, J. L. Qi, Y. fan et al., "Particle crushing of frozen sand under triaxial compression," *Chinese Journal of Geotechnical Engineering*, vol. 37, no. 3, pp. 544–550, 2015.

[12] T. Fukumoto, "Particle breakage characteristics of granular soils," *Soils and Foundations*, vol. 32, no. 1, pp. 26–40, 2008.

[13] R. J. Marsal, "Large scale testing of rockfill materials," *Journal of the Soil Mechanics and Foundations Division*, vol. 94, pp. 1042–1047, 1967.

[14] K. L. Lee, "Drained strength characteristics of sands," *Journal of the Soil Mechanics and Foundation Division*, vol. 93, no. 6, pp. 117–141, 1967.

[15] A. S. Vesic and G. W. Clough, "Behavior of granular material under high stress," *ASCE Journal of the Soil Mechanics and Foundations Division*, vol. 94, no. SM3, pp. 661–688, 1968.

[16] N. Miura, S. O-Hara, and S. O-Hara, "Particle-crushing of a decomposed granite soil under shear stresses," *Soils and Foundations*, vol. 19, no. 3, pp. 1–14, 1979.

[17] Q. Guo, "Experimental study on shear strength characteristics of coarse-grained soil," *Journal of Hydraulic Engineering*, no. 5, pp. 61–67, 1987.

[18] M. Jin and Z. Qu, "Stress-strain behaviour of glacial till under high confining pressure," *Journal of Sichuan University: Engineering Science Edition*, no. 1, pp. 17–22, 1989, in Chinese.

[19] R. Wang and J. Sun, "Damage slip coupling analysis of undrained characters of calcareous sand," *Journal of Hydraulic Engineering*, vol. 33, no. 7, pp. 75–78, 2002.

[20] C. Chavez and E. E. Alonso, "A constitutive model for crushed granular aggregates which includes suction effects," *Soils and Foundations*, vol. 43, no. 4, pp. 215–227, 2008.

[21] M. Zhankuan, G. Li, and T. Chen, "Constitutive model for rockfill material considering grain crushing," *Chinese Journal of Geotechnical Engineering*, vol. 29, no. 12, pp. 1865–1869, 2007.

[22] M. Zhankuan, G. Li, and S. Chen, "Constitutive model for coarse granular materials based on breakage energy," *Chinese*

Journal of Geotechnical Engineering, vol. 34, no. 10, pp. 1801–1811, 2012.

[23] T.-S. Ueng and T.-J. Chen, "Energy aspects of particle breakage in drained shear of sands," *Géotechnique*, vol. 50, no. 1, pp. 65–72, 2000.

[24] P. W. Rowe, "The stress-dilatancy relation for static equilibrium of an assembly of particles in contact," *Proceedings of the Royal Society of London. Series A. Mathematical and Physical Sciences*, vol. 269, no. 1339, pp. 500–527, 1962.

[25] B. Indraratna and W. Salim, "Modeling of particle breakage of coarse aggregates incorporating strength and dilatancy," *Proceedings of the Institution of Civil Engineers—Geotechnical Engineering*, vol. 155, no. 4, pp. 243–252, 2002.

[26] S. Chi and Y. Jia, "Correction of the energy Rowe's stress-dilatancy model modified for energy dissipation of particle breakage," *Chinese Journal of Geotechnical Engineering*, vol. 27, no. 11, pp. 1266–1269, 2005.

[27] Z. Li, *Constitutive Model for Coarse Granular Soil Incorporating Particle Breakage*, Dalian University of Technology, Dalian, China, 2007.

[28] P. V. Lade, "Elasto-plastic stress-strain theory for cohesionless soil with curved yield surfaces," *International Journal of Solids and Structures*, vol. 13, no. 11, pp. 1019–1035, 1977.

[29] P. A. Vemeer, "A double hardening model for sand," *Geotechnique*, vol. 28, no. 4, pp. 413–433, 1978.

[30] Z. Z. A. Yin, "Constitutive model with two yield surfaces for soils," in *Proceedings of The Sixth International Conference on Numerical Methods In Geomechanics*, vol. 1-3, Innsbruck, Austria, April 1988.

[31] Z. Shen, ""Nanshui" double yield surface model and its application," in *Proceedings of Academic Symposium on Soil Mechanics and Foundation Engineering and Geotechnical Engineering on Both sIdes of the Taiwan Strait*, Xi'an, China, 1994.

[32] B. Zhang, Y. Jia, and Z. Zhang, "Modified Rowe's dilatancy law of rockfill and Shen Zhujiang's double yield surfaces elastoplastic model," *Chinese Journal of Geotechnical Engineering*, vol. 29, no. 10, pp. 1443–1448, 2007.

[33] G. Luo and J. Zhang, "Improvement of Duncan-Chang nonlinear model and Shen Zhujiang's elastoplastic model for granular soils," *Rock and Soil Mechanics*, vol. 25, no. 6, pp. 887–890, 2004.

[34] T. Wang, S. Chen, and Z. Fu, "Two modifications to the shen Zhujiang's double yield surface model," *Journal of Tongji University(Natural Science)*, vol. 44, no. 3, pp. 362–368, 2016.

[35] W. Ma and Z. Wu, "Analysis of microstructural changes in frozen sandy soil under confining pressures using scaning electronic microscop," *Journal of Glaciology and Geocaryology*, vol. 17, no. 2, pp. 152–158, 1995.

[36] Y. Zheng, W. Ma, and B. Hui, "Impact of freezing and thawing cycles on the structures of soil and a quantitative approach," *Journal of Glaciology and Geocryology*, vol. 37, no. 1, pp. 132–137, 2015.

[37] E. Guyon and J.-P. Troadec, *Du Sac de Billes au tas De Sable*, Editions Odile JACOB Sciences, Paris, France, 1994.

[38] M. A. Elsohby, "Elastic behavior of sand," *Proceedings of ASCE*, vol. 95, 1969.

[39] M. Hassanlourad, H. Salehzadeh, and H. Shahnazari, "Dilation and particle breakage effects on the shear strength of calcareous sands based on energy aspects," *Cytometry Part A the Journal of the International Society for Analytical Cytology*, vol. 6, no. 2, pp. 108–119, 2008.

[40] K. H. Roscoe, "On the generalised stress-strain behaviour of wet clay," *Engineering Plasticity*, pp. 535–609, 1968.